

ENCYCLOPEDIA OF

MOLECULAR BIOLOGY

VOLUME 4

Thomas E. Creighton

*European Molecular Biology Laboratory
London, England*



A Wiley-Interscience Publication

John Wiley & Sons, Inc.

New York / Chichester / Weinheim / Brisbane / Singapore / Toronto

This book is printed on acid-free paper. ©

Copyright © 1999 by John Wiley & Sons, Inc.

All rights reserved. Published simultaneously

No part of this publication may be reproduced

in any form or by any means, electronic, mech-

anically, except as permitted under Sections

107 and 108 of the Copyright Act of 1976 without

permission in writing from the publisher.

For permission to reproduce contact the

Wiley Permissions Department, 605 Third Avenue,

New York, NY 10158-0001.

For ordering and customer service, call 1-800-CALL-WILEY.

E-Mail: PERMREQ@WILEY.COM

Printed in the United States of America

10 9 8 7 6 5 4 3 2 1

ISBN 0-471-15302-8 (alk. paper)

0471-15302-8 (hbk. paper)

0471-15302-8 (pbk. paper)

0471-15302-8 (pbk. paper)

0471-15302-8 (pbk. paper)

0471-15302-8 (pbk. paper)

0471-15302-8 (pbk. paper)

0058378

ENCYCLOPEDIA OF

MOLECULAR

BIOLOGY

VOLUME 4

Edited by Thomas J. Murray and Maxwell J. Meselson

Thomas E. Creighton

European Molecular Biology Laboratory
London, England

Editorial Board
Allan M. Campbell
Stanford University

Akiyoshi Wada
Sagami Chemical Research Center

Peter Wright
The Scripps Research Institute

Series Editor
Larry Hood
University of Washington

This book is printed on acid-free paper. ©

Copyright © 1999 by John Wiley & Sons, Inc.

All rights reserved. Published simultaneously in Canada.

No part of this publication may be reproduced, stored in a retrieval system or transmitted in any form or by any means, electronic, mechanical, photocopying, recording, scanning or otherwise, except as permitted under Sections 107 or 108 of the 1976 United States Copyright Act, without either the prior written permission of the Publisher, or authorization through payment of the appropriate per-copy fee to the Copyright Clearance Center, 222 Rosewood Drive, Danvers, MA 01923, (508) 750-8400, fax (508) 750-4744. Requests to the Publisher for permission should be addressed to the Permissions Department, John Wiley & Sons, Inc., 605 Third Avenue, New York, NY 10158-0012, (212) 850-6011, fax (212) 850-6008, E-Mail: PERMREQ@WILEY.COM.

For ordering and customer service, call 1-800-CALL-WILEY.

Library of Congress Cataloging-in-Publication Data:

Creighton, Thomas E., 1940-

The encyclopedia of molecular biology / Thomas E. Creighton.
p. cm.

Includes index.

ISBN 0-471-15302-8 (alk. paper)

1. Molecular biology—Encyclopedias. I. Title.

QH506.C74 1999

572.8'03—dc21

99-11575
CIP

Printed in the United States of America.

10 9 8 7 6 5 4 3 2 1



8726500



ENCYCLOPEDIA OF

WILEY BIOTECHNOLOGY ENCYCLOPEDIA

ENCYCLOPEDIA OF

MOLECULAR BIOLOGY

VOLUME 4

Encyclopedia of Bioprocess Technology: Fermentation
Edited by Michael C. Flickinger and Stephen W.
Encyclopedia of Molecular Biology
Edited by Thomas E. Creighton
Encyclopedia of Cell Technology
Edited by Raymond E. Spier

Encyclopedia of Clinical, Legal, and Policy Issues in Biotechnology
Edited by Thomas J. Murray and Maxwell J. Mehlman

Thomas E. Creighton

European Molecular Biology Laboratory
London, England

ENCYCLOPEDIA OF MOLECULAR BIOLOGY

Editorial Board
Allan M. Campbell
Stanford University

Akiyoshi Wada
Sagami Chemical Research Center

Peter Wright
The Scripps Research Institute

Gordon G. Hammes
Duke University Medical Center

Series Editor
Leroy Hood
University of Washington

Aaron Klug
MRC Laboratory of Molecular Biology

Editorial Staff
Publisher: Jacqueline I. Kroschwitz
Editor: Glenn Collins

J. Robert Lehman
Stanford University School of Medicine

Managing Editor: John Sallami
Assistant Managing Editor: Brendan Vitorio

Paul Schimmel
Massachusetts Institute of Technology

John Tooz
Imperial Cancer Research Fund

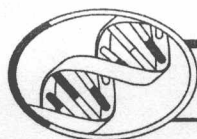
Editorial Assistant: Tugh Kelly



A Wiley-Interscience Publication

John Wiley & Sons, Inc.

New York / Chichester / Weinheim / Brisbane / Singapore / Toronto



WILEY BIOTECHNOLOGY ENCYCLOPEDIAS

Encyclopedia of Bioprocess Technology: Fermentation, Biocatalysis, and Bioseparation

Edited by Michael C. Flickinger and Stephen W. Drew

Encyclopedia of Molecular Biology

Edited by Thomas E. Creighton

Encyclopedia of Cell Technology

Edited by Raymond E. Spier

Encyclopedia of Ethical, Legal, and Policy Issues in Biotechnology

Edited by Thomas J. Murray and Maxwell J. Mehlman

ENCYCLOPEDIA OF MOLECULAR BIOLOGY

Editorial Board

Allan M. Campbell
Stanford University

Gordon G. Hammes
Duke University Medical Center

Aaron Klug
MRC Laboratory of Molecular Biology

I. Robert Lehman
Stanford University School of Medicine

Paul Schimmel
Massachusetts Institute of Technology

John Tooze
Imperial Cancer Research Fund

Akiyoshi Wada
Sagami Chemical Research Center

Peter Wright
The Scripps Research Institute

Series Editor
Leroy Hood
University of Washington

Editorial Staff
Publisher: **Jacqueline I. Kroschwitz**

Editor: **Glenn Collins**

Managing Editor: **John Sollami**

Assistant Managing Editor: **Brendan Vilardo**

Editorial Assistant: **Hugh Kelly**

ENCYCLOPEDIA OF

MOLECULAR
BIOLOGY

VOLUME 4

The R -factor is why is presenting a model is determined. If this were not the case, the models in the crystal structure were accurately known, the calculated the amplitude of the reflections would be equal to the observed amplitude. In practice this ideal situation is never achieved. The difference between the model's and the observed amplitudes, averaged over all of the measured reflections, is expressed as the crystallographic R -factor or reliability or residual index R :

$$R = \frac{\sum |F_o| - \sum |F_c|}{\sum |F_o|}$$

or alternatively

$$R = \frac{\sum |F_o| - \sum |F_c|}{\sum |F_o|} \times 100\%$$

where k is a factor scaling the F_{max} to the F_{min} . If the atoms were to be placed entirely at random in a non-centrosymmetrical structure like a protein, R would have the value 0.59. For correct structures refined to, for example, 2.0 Å resolution, the R -factor is of the order of 0.20. If it is much higher, the structure is not likely to be correct.

A better estimate for the reliability of a protein structure is the free R -factor (R_{free}). It is calculated for a random selection of 5 to 10% of the observed reflections. These reflections are not used in the refinement, so refining and testing are completely independent.

BIBLIOGRAPHY

1. A. T. Brünger (1982) *Acta Crystallogr.* D39, 24-36.

Suggestion for Further Reading

1. Drenth (1956) *Principles of Protein X-ray Crystallography*, Springer, New York.

RACEMIC AND RACEMIZATION

VERNON ANDERSON

A mixture containing equal amounts of both enantiomers of a compound is a **racemic mixture**, which may also be called

racemate. An example of a racemic mixture is tartaric acid, which is a mixture of two enantiomers. This compound is now known as (2R,3R)-tartaric acid. When a chiral compound is formed by the reaction of two achiral reactants, the product must be a racemic mixture (2). An example of such a reaction is the reduction of the imine of pyruvate by sodium borohydride as shown in Figure 1. The product, alanine, is chiral, but both enantiomers must be generated in identical amounts.

The process of separating a racemic mixture into its two enantiomers is called **racemization**. A process that catalyzes the interconversion of enantiomers, or a racemization, will necessarily result in a racemic mixture being formed. This must be so because the free energy of formation of the two enantiomers, in the absence of any other chiral compound, must be identical. During the chemical process of peptide synthesis, racemization of the activated amino acid derivatives has been a major problem. Enzymes, such as proline racemase, will racemize a solution of either the L- or D-enantiomer by catalyzing the interconversion of the two enantiomers, generating a racemic mixture of the substrate.

BIBLIOGRAPHY

1. L. Pasteur (1858) *Pharmazie*, J. XIII, LII.
2. E. L. Eliel (1962) *Stereochemistry of Carbon Compounds*, McGraw-Hill, New York, Chap. 4.

Suggestion for Further Reading

1. March, J. (1985) *Advanced Organic Chemistry*, Wiley-Interscience, New York, pp. 102-107.

RADIATION HYBRID

ALAN P. WOLFE

The fusion of somatic cells from different species to create somatic cell hybrids has provided an exceptionally useful tool for mapping of genes to particular chromosomes because the chromosomes of one species are always progressively lost in such interspecific somatic cell hybrids (1). Using hybrid cell lines, it is also possible to use recognizable chromosome break points to localize genetic loci more accurately. This process is greatly facilitated by inducing chromosome breaks with

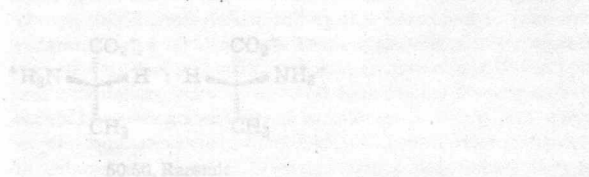


Figure 1. Generating the chiral products L- and D-alanine from achiral reactants. The two products are produced in equal amounts, to give a racemic mixture of DL-alanine.

R-FACTOR (CRYSTALLOGRAPHIC)

JAN DRENTH

The final result in **X-ray crystallography** is presenting a molecular model of the structure being determined. If this were an ideal model and if the packing of the models in the crystal structure were accurately known, the calculated the amplitude of the **structure factor** F_{calc} would be equal to the observed amplitude F_{obs} for each reflection. In practice this ideal situation does not exist, and the difference between the two values indicates model's inadequacies. This difference, averaged over all of the measured reflections, is expressed as the crystallographic R-factor or residual index R :

$$R = \frac{\sum_{hkl} |F_{\text{obs}}| - k|F_{\text{calc}}|}{\sum_{hkl} |F_{\text{obs}}|}$$

or alternatively

$$R = \frac{\sum_{hkl} |F_{\text{obs}}| - k|F_{\text{calc}}|}{\sum_{hkl} |F_{\text{obs}}|} \times 100\%$$

where k is a factor scaling the F_{calc} to the F_{obs} 's.

If the atoms were to be placed entirely at random in a non-centrosymmetrical structure like a protein, R would have the value 0.59. For correct structures refined to, for example, 2.0 Å resolution, the R -factor is of the order of 0.20. If it is much higher, the structure is not likely to be correct.

A better estimate for the reliability of a protein structure is the free R -factor (1). It is calculated for a random selection of 5 to 10% of the observed reflections. These reflections are not used in the refinement, so refining and testing are completely independent.

BIBLIOGRAPHY

1. A. T. Brünger (1993) *Acta Crystallogr.* **D49**, 24–36.

Suggestion for Further Reading

- J. Drenth (1999) *Principles of Protein X-ray Crystallography*, Springer, New York.

RACEMIC AND RACEMIZATION

VERNON ANDERSON

A mixture containing equal amounts of both **enantiomers** of a compound is a **racemic mixture**, which may also be called

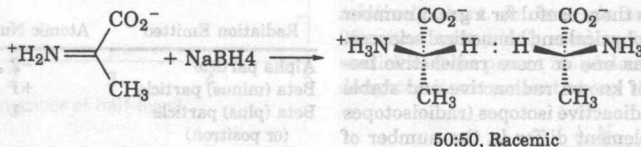


Figure 1. Generating the chiral products L- and D-alanine from achiral reactants. The two products are produced in equal amounts, to give a racemic mixture of DL-alanine.

a **racemate**. The original compound identified as containing equal parts of two enantiomers was racemic acid as isolated from grapes (1). This compound is now known as (\pm) tartaric acid. When a **chiral** compound is formed by the reaction of two achiral reactants, the product must be a racemic mixture (2). An example of such a reaction is the reduction of the imine of pyruvate by sodium borohydride as shown in Figure 1. The product alanine is chiral, but both enantiomers must be generated in identical amounts.

The process of separating a racemic mixture into its two enantiomeric components is called **racemic resolution**. Any process that catalyzes the interconversion of enantiomers, ie, a **racemization**, will necessarily result in a racemic mixture being formed. This must be so because the free energy of formation of the two enantiomers, in the absence of any other chiral compound, must be identical. During the chemical process of **peptide synthesis**, racemization of the activated amino acid derivatives has been a major problem. **Enzymes**, such as proline racemase, will racemize a solution of either the L- or D-enantiomer by catalyzing the interconversion of the two enantiomers, generating a racemic mixture of the substrate.

BIBLIOGRAPHY

1. L. Pasteur (1853) *Pharmacol. J.* **XIII**, 111.
2. E. L. Eliel (1962) *Stereochemistry of Carbon Compounds*, McGraw-Hill, New York, Chap. 4.

Suggestion for Further Reading

- March, J. (1985) *Advanced Organic Chemistry*, Wiley-Interscience, New York, pp. 102–107.

RADIATION HYBRID

ALAN P. WOLFFE

The fusion of **somatic cells** from different species to create somatic cell hybrids has provided an exceptionally useful tool for mapping of genes to particular **chromosomes** because the chromosomes of one species are always progressively lost in such interspecific somatic cell hybrids (1). Using hybrid cell lines, it is also possible to use recognizable chromosome break-points to localize genetic loci more accurately. This process is greatly facilitated by inducing chromosome breaks with

radiation (2). This technique uses a somatic cell hybrid between a rodent and a human cell that contains a single human chromosome, all of the rodent chromosomes, and a selectable marker that confers resistance to the antibiotic **neomycin**. The chromosomes in this hybrid cell line are fragmented by irradiation such that cell death normally occurs. However, the irradiated hybrid cell line is rescued by fusion with another rodent cell line that is neomycin-sensitive. Growth in neomycin allows selection to operate in favor of the resulting radiation hybrid cell lines, rather than the neomycin-sensitive unfused cell line. Fragments of the human chromosomes are retained and incorporated into the rodent cell chromosomes. The different radiation hybrid cell lines generated in this way can be examined for the presence or absence of molecular markers from the human chromosome.

The production of radiation hybrids has provided a useful methodology for mapping how close genes are in the human chromosome. Two genes that are close together remain together following radiation, whereas those that are far apart are separated. By estimating the frequency of separation, it is possible to build up a physical map of the chromosome providing gene order and distance (3).

BIBLIOGRAPHY

1. R. L. Stallings and M. J. Siciliano (1981) *Somat. Cell Genet.* **7**, 683–697.
2. S. J. Goss and H. Harris (1977) *J. Cell Sci.* **25**, 17–28.
3. M. A. Walter and P. N. Goodfellow (1993) *Trends Genet.* **9**, 352–356.

Suggestion for Further Reading

M. S. Clark and W. J. Wall (1996) *Chromosomes. The Complex Code*, Chapman and Hall, London.

RADIOACTIVITY

D. R. FISHER

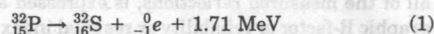
Radioactivity is the property of certain elements to undergo spontaneous transformation of their atomic nuclei, the release of energy, and the formation of new elements (decay products). Radioactive nuclei are unstable and seek a more stable configuration by releasing energetic particles or photons of energy. These particles may include alpha particles, beta particles, and positrons. Photons include gamma rays, X rays, and neutrinos, which are discrete quanta of energy without mass or charge. These emissions impart energy to matter by creating tracks of ionized molecules. The emission of charged particles or gamma rays may be measured with radiation detectors. This property of radioactive materials makes them useful for a great number of practical applications in the physical and biomedical sciences.

Every chemical element has one or more radioactive isotopes, and the total number of known radioactive and stable isotopes is more than 1500. Radioactive isotopes (radioisotopes or radionuclides) of a given element differ in the number of neutrons in the nucleus and, hence, in total atomic mass. A radioactive label (radiolabel) is a radionuclide or radioisotope in a chemical compound that replaces a stable isotope of the

same element. It is used to mark the compound for detection by instruments that measure radioactivity. Radioactive labeling is useful for tracking the uptake, retention, metabolism, or clearance of chemical compounds, or for investigating metabolic pathways, **enzyme** kinetics, or chemical reactions. Radioactive labels are sometimes called radioactive tracers.

The radioactivity of a particular nuclide is determined by the configuration of its atomic nucleus and is independent of the chemical and physical state of the radioisotope and its environment (temperature and pressure). Radioactivity takes many different forms. The process of radioactive disintegration results in changes to the nucleus in atomic number and in its number of nucleons (protons plus neutrons), as indicated in Table 1.

An example of radioactive transformation is the decay of phosphorus-32 to sulfur-32 by emission of a beta (minus) particle (or electron), ${}_{-1}^0e$:



Beta decay and positron emission also are accompanied by emission of energy in the form of a nonionizing neutrino. Decay schemes for radionuclides may be complex.

The total energy of the gamma rays and charged particles emitted during radioactive decay is equivalent to the net decrease in the rest mass of the disintegrating atom as it changes from parent to decay product. Its energy, momentum, and electronic charge are conserved. The emitted energy is either kinetic energy of particles in motion or quantum energy of photons, each of which degrades into heat. The ionization of matter through which radiation passes may result in direct or indirect chemical changes and radiation damage.

HALF-LIFE

The transformation kinetics of radioactive decay are unique to each radioisotope, and each has its own characteristic, constant decay rate. The time required for any given radioisotope to decay in amount to one-half of its original amount is a measure of the rate at which radioactive transformation takes place. The physical half-life ($t_{1/2}$) of a radioactive atom may range from fractions of a second to billions of years and is unique to each radionuclide. Naturally existing radionuclides have long physical half-lives or are created by the decay of radioisotopes with long half-lives.

If N is the number of identical radioactive atoms and λ is the radioactive decay constant (s^{-1} ; reciprocal seconds), then $1/\lambda$ is

Table 1. Changes in Atomic Number and the Number of Nucleons by Radioactive Transformation*

Radiation Emitted	Atomic Number	Change in
		Number of Nucleons
Alpha particle	-2	-4
Beta (minus) particle	+1	0
Beta (plus) particle (or positron)	-1	0
Gamma or X ray	0	0

* From F. H. Attix (1986) *Introduction to Radiological Physics and Radiation Dosimetry*, John Wiley & Sons, New York.

the activity, and the rate of change in N at any time t is equal to the activity

$$\frac{dN}{dt} = \lambda N \quad (2)$$

Integrating from $t = 0$ (when $N = N_0$), we obtain

$$\int_{N_0}^N \frac{dN}{N} = - \int_0^t \lambda dt \quad (3)$$

$$\therefore \ln N - \ln N_0 = -(\lambda t - 0) \quad (4)$$

$$\ln \frac{N}{N_0} = -\lambda t \quad (5)$$

$$\frac{N}{N_0} = e^{-\lambda t} \text{ or } N = N_0 e^{-\lambda t} \quad (6)$$

Equation 6 describes the observed law of radioactive decay and is a formula that is useful for determining the amount of a radioactive material remaining after a period of time t (Fig. 1).

The unit of activity was originally the curie (Ci), the number of disintegrations per second taking place in 1 g of ^{226}Ra , where

$$1 \text{ Ci} = 3.7 \times 10^{10} \text{ disintegrations per second} \quad (7)$$

In recent years, the curie has been replaced with the special S.I. unit becquerel (Bq), which is one disintegration per second. However, the units of curie, millicurie, and microcurie are still commonly used.

$$1 \text{ Ci} = 3.7 \times 10^{10} \text{ Bq} \quad (8)$$

$$1 \text{ mCi} = 3.7 \times 10^7 \text{ Bq} \quad (9)$$

$$1 \mu\text{Ci} = 3.7 \times 10^4 \text{ Bq} \quad (10)$$

MEAN LIFE

The mean life of a radioactive material is the time required for an original amount N_0 to decay to $1/e$ of the original amount. Thus

$$\frac{N}{N_0} = \frac{1}{e} = 0.3679 = e^{-\lambda \tau} \quad (11)$$

where τ is the mean life (s) of the material:

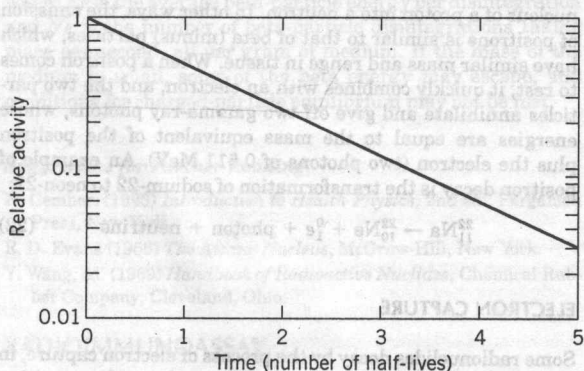


Figure 1. Semilog plot of the exponential decay of a radioactive material in terms of the number of half-lives that have transpired.

$$\ln e^{-1} = -1 = -\lambda \tau \quad (12)$$

$$\tau (\text{mean life}) = \frac{1}{\lambda} = 1.443 T_{1/2} \quad (13)$$

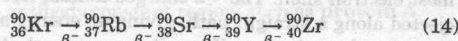
SPECIFIC ACTIVITY

The specific activity (Bq/g) is the activity (Bq) of a radioactive material per unit mass (g) or volume. The mass or volume may refer to the element itself or to the medium in which the radioactive material is contained. For example, the specific activity of a carbon-14-labeled compound is the radioactivity (Bq) of the carbon-14 divided by the total mass of all the compound molecules in a given volume.

SERIAL TRANSFORMATION

If the decay products of a radioactive material are themselves radioactive, a decay chain is said to exist. The ingrowth of the first decay product is dependent on the rate of decay of the parent, and so forth through each daughter-product decay, until a stable isotope finally ends the chain. Three natural radioactive series exhibit long decay chains of successive members: the thorium-232 chain, with 12 members, concludes with stable lead-208; the uranium-238 series, with 19 members, concludes with stable lead-206, and the uranium-235 series, with 14 members, concludes with stable lead-207. A fourth series starting with plutonium-241, with 15 members and concluding with bismuth-209, has been created artificially. Each radioactive isotope of a decay chain emits alpha or beta particles and possibly also gamma rays.

An example of serial transformation is given by the decay of krypton-90, a fission product of uranium-235. Each step involves beta (minus) decay:



The rate of formation of a daughter radionuclide, or the number of daughter atoms present (N_d) from its parent (N_p), is equal to the rate of formation of the parent; however, each will have different decay rates. If the half-life of the parent (p) is much longer than that of the daughter (d) and only the parent is present at time zero ($t = 0$), the formation of the daughter product is described by secular equilibrium:

$$(N_d) = \frac{\lambda_p N_p}{\lambda_d} (1 - e^{-\lambda_d t}) \quad (15)$$

At equilibrium, $\lambda_p N_p = \lambda_d N_d$, and the activities of each radioactive member are equal ($A_p = A_d$). A state of transient equilibrium exists when the half-life of the parent is somewhat greater than that of the daughter and both half-lives are relatively short. An example is the ingrowth of technetium-99m (the most widely used radioisotope in diagnostic nuclear medicine) from parent molybdenum-99 (Fig. 2). The number of daughter atoms present at any time t is given by

$$(N_d) = \frac{\lambda_p N_p}{\lambda_d - \lambda_p} (e^{-\lambda_p t} - e^{-\lambda_d t}) \quad (16)$$

When transient equilibrium occurs, the daughter radioisotope undergoes radioactive transformation at the same rate as it

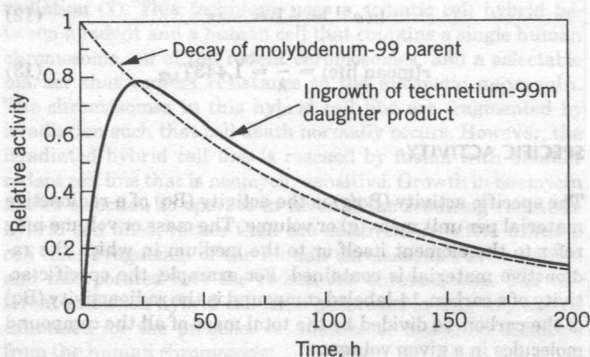
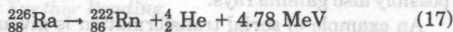


Figure 2. Radioactive decay of molybdenum-99 and ingrowth of technetium-99m with time (an example of *transient equilibrium*). The amount of radioactivity from each isotope is plotted as a function of time.

is produced, decreasing in amount with time according to the decay rate of its parent, as shown in Figure 2.

ALPHA PARTICLES

An alpha particle is equivalent to a helium nucleus (two protons plus two neutrons). Alpha decay usually occurs in nuclei of heavy radioactive atoms. An example of alpha decay is the transformation of radium-226 to radon-222 with a half-life of 1600 years:



Alpha particles are essentially monoenergetic. During formation of radon-222, two electrons are ejected from the outermost electron shell. The +2 charged helium (He^{2+}) nucleus is ejected along a straight path, giving up energy and producing ion pairs along the way. When it comes to rest, it captures two electrons from its environment and becomes a stable, neutral helium atom. Most of the 4.78 MeV is given up to the absorbing medium as kinetic energy. During 95% of the time there is emission of a 4.70 MeV alpha particle and 0.08 MeV as radon-222 recoil energy. In the remaining 5% of the time there is emission of a 4.6-MeV alpha particle, and 0.18 MeV is given off as gamma rays.

The range of the alpha particle in a unit-density medium is only a few micrometers. The thickness of skin or a sheet of paper is sufficient to prevent most alpha-particle penetration. The range, R , of an alpha particle in air at 0°C and 760 mmHg pressure may be estimated from

$$R(\text{cm}) = 0.56E_\alpha (\text{MeV}) \text{ for } E < 4 \text{ MeV} \quad (18)$$

$$R(\text{cm}) = 1.24 E_\alpha (\text{MeV}) - 2.62 \text{ for } 4 < E < 8 \text{ MeV} \quad (19)$$

The range of alpha particles in media other than air may be estimated from

$$R_m(\text{mg}/\text{cm}^2) = 0.56A^{0.33}R_{\text{air}} \quad (20)$$

where A is the atomic number of the absorbing medium and R_{air} is the range of the alpha particle in air (cm).

Alpha-particle tracks may give rise to low energy, secondary electron tracks, called *delta rays*, which radiate

outward to distances of tens of nanometers from the primary particle track.

BETA PARTICLES

Beta particles are electrons that are ejected from the nucleus of an unstable, beta-emitting atom. Beta particles carry a single negative charge and small mass (only about 1/1800th that of a proton or neutron). Beta emission appears as the change in a nucleus of one neutron into a proton, and occurs among radionuclides with greater numbers of neutrons than protons in the nucleus. An example was given in equation 1 above.

Beta particles are not monoenergetic, but rather are emitted with a continuous energy distribution, ranging from near zero to the theoretical maximum energy. To comply with the law of conservation of energy, each beta particle is accompanied by emission of a neutrino, whose energy makes up the difference between the theoretical maximum energy of the beta particle and its observed kinetic energy. Gamma rays may accompany beta emission in order to reach the ground energy state of the daughter product. For example, potassium-42 decays 82% of the time by a maximum energy of 3.55 MeV to calcium-42, and 18% of the time by a maximum energy of 2.04 MeV, together with a gamma ray of 1.53 MeV.

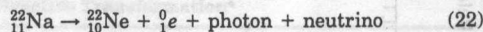
When beta particles slow to rest, they transfer a negative charge to the absorber. Their range is a few millimeters in unit-density tissue. The beta energy range may be measured by adding successively thicker absorbers until a count rate cannot be detected. An absorber that stops one-half the beta particles is about one-eighth the range of beta particles. An estimate of the range of beta particles may be obtained from

$$R(\text{mg}/\text{cm}^2) = 412E^{1.265 - 0.0954 \ln E} \quad (21)$$

for electron energies between 0.01 and 2.5 (MeV).

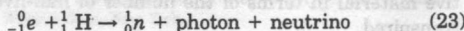
POSITRONS

Positrons are positively charged electrons that are emitted from atomic nuclei where the neutron:proton ratio is low and sufficient energy is not available for alpha-particle decay. Positron emission represents the transformation within the nucleus of a proton into a neutron. In other ways, the emission of positrons is similar to that of beta (minus) particles, which have similar mass and range in tissue. When a positron comes to rest, it quickly combines with an electron, and the two particles annihilate and give off two gamma-ray photons, whose energies are equal to the mass equivalent of the positron plus the electron (two photons of 0.511 MeV). An example of positron decay is the transformation of sodium-22 to neon-22:



ELECTRON CAPTURE

Some radionuclides decay by the process of electron capture, in which a K orbital electron is captured into the nucleus, uniting with a proton or hydrogen nucleus and changing it into a neutron:



When an atom decays by electron capture, a characteristic X ray (photon) is emitted as an electron from an outer orbit falls into the energy level of the captured electron.

GAMMA RAYS

Gamma rays are monoenergetic photons or quanta of energy with discrete frequency that are emitted from the nucleus during radioactive decay to remove excess energy. Like X rays, gamma rays are highly penetrating electromagnetic photons of energy. Gamma rays usually accompany beta decay and always accompany positron decay. Gamma rays are attenuated by matter, and the efficiency of the shielding increases with atomic number.

INTERNAL CONVERSION

Radioactive decay by internal conversion takes place when an unstable nucleus of a gamma-emitting nucleus gives off excess excitation energy by imparting energy to an orbital *K*- or *L*-shell electron, ejecting it from the atom. Characteristic X rays are emitted as outer-shell orbital electrons collapse inward to fill vacant energy levels produced by ejected electrons. If the characteristic X rays are absorbed by an inner orbital electron, internal conversion may take place, ejecting the electron (called an Auger electron).

RADIATION ABSORBED DOSE

Radiation absorbed dose is the energy deposited by radiation per unit mass of the absorbing medium. The radiation absorbed dose in units of gray (Gy) to a unit-density medium containing an alpha-emitter is

$$D(\text{Gy}) = 1.61 \times 10^{-10} E_{\alpha}(\text{MeV}) \frac{N_{\alpha}}{g} \quad (24)$$

where E_{α} is the average alpha-particle energy, N_{α} is the number of alpha particles emitted in the medium, and g is the mass of the medium.

The radiation absorbed dose rate (D° , in grays per second) from a beta-emitting radioisotope under conditions of charged-particle equilibrium can be estimated from

$$D^{\circ}(\text{Gy/s}) = 1.61 \times 10^{-10} E_{\beta}(\text{MeV}) \frac{N_{\beta}}{g} \quad (25)$$

where E_{β} is the average beta-particle energy per disintegration and N_{β} is the number of beta-particle disintegrations taking place per second, all per gram of medium. If the mass of the medium is small, some of the beta energy may escape, and conditions for charged-particle equilibrium may not be met.

Suggestions for Further Reading

- H. Cember. (1983) *Introduction to Health Physics*, 2nd ed., Pergamon Press, New York.
- R. D. Evans (1955) *The Atomic Nucleus*, McGraw-Hill, New York.
- Y. Wang, ed. (1969) *Handbook of Radioactive Nuclides*, Chemical Rubber Company, Cleveland, Ohio.

RADIOIMMUNOASSAY

J. FOOTE

Radioimmunoassay (RIA) is a technique for determining the content of a particular molecule in a sample, based on

displacement of a radioactive **antigen** from an **antibody** or **antiserum**. Berson and Yalow and their colleagues developed the RIA method, and first applied it to the assay of human and animal **insulins** in plasma (1,2). RIA has subsequently been used most extensively in endocrinology, as the technique is sufficiently sensitive for detection of vanishingly small quantities of **hormones**, but it is by no means restricted to hormones and has also been applied to all classes of biomolecule. Many modifications of the original technique are in common use. Here we discuss the classical RIA and several of the most common variations.

CLASSIC RIA

Materials necessary for a classic RIA are:

- The unknown, that is, a sample of a chemically known antigen whose concentration is unknown and to be determined.
- Standards for calibrating the assay. These must be chemically identical to the unknown and of known concentration.
- A polyclonal or **monoclonal antibody** preparation that binds the unknown specifically.
- A **radiolabeled** ligand, termed a *tracer*, that binds to the antibody competitively with the unknown. Most often the tracer is chemically identical to the unknown, except for the radioactive tag, which usually is, or contains, an **iodine isotope**. Identity is not required, however, as long as binding of the tracer and the unknown to the antibody are mutually exclusive.
- A means for rapidly separating bound and free tracer. Separation is often accomplished using an antiglobulin antibody to **immunoprecipitate** the antibody-tracer complex, or an immobilized affinity adsorbent that reacts with the antibody constant region, such as **protein A**.

The RIA is initiated by adding the antibody to mixtures of a constant amount of tracer and increasing amounts of either the calibration standard or the unknown. Ideally, the tracer will be present in negligible molar quantity, relative to the **ligand-binding** capacity of the antibody, so that saturating half of the antibody sites with standard or unknown will displace half of the tracer. The necessary controls are (1) antibody added to tracer with a large excess of the calibration standard, to measure background radioactivity under conditions of complete tracer displacement, and (2) antibody added to tracer alone, to measure the radioactivity bound when no displacement occurs. After a suitable time for equilibration of the mixtures, bound and free tracer are separated, and one or both are measured. A dose-response curve, based on the calibration standards, can be plotted directly as the fraction of bound tracer retained or displaced as a function of the amount of standard added. This fraction is relative to the quantity of tracer bound in the absence of added unlabeled standard, not to the total amount of tracer added to the reaction. An example of such a direct plot is shown in Figure 1.

A preferable treatment of data is to construct a logit-log plot (3). The logit transformation for a fraction f is defined as

$$\text{logit } f = \ln \frac{f}{1-f} \quad (1)$$

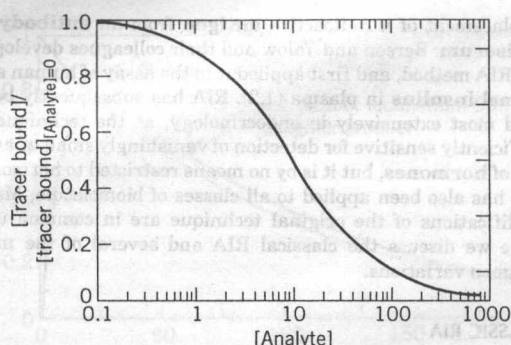


Figure 1. Dose-response curve typical of a classic RIA. Addition of increasing amounts of ligand progressively displaces the radioactive tracer from the antibody in the assay, generating an S-shaped curve. The abscissa in the figure is a concentration scale in units of the amount of unlabeled antigen added. The ordinate is a fractional scale, where 1.0 corresponds to the tracer bound to antibody in the absence of added antigen.

For RIA data, this corresponds to

$$\text{logit } f = \ln \frac{\text{fraction of tracer retained}}{\text{fraction of tracer displaced}} \quad (2)$$

A plot of $\text{logit } f$ versus \log_{10} (standard) is often linear over much of its range; hence it is more easily analyzed than the S-shaped direct plot.

On the basis of the dose-response behavior of the standards, the amount of tracer displaced by the unknown can be related graphically or algebraically to the quantity of antigen that must have been present in the unknown. Software for statistical analysis of RIA data is also widely available.

SOLID-PHASE RIA

This method is similar to the classical RIA, but with a great practical simplification: as the first step of the assay, the antibody is adsorbed to the surface of plastic assay tubes (4). (Other media such as beads and disks can also be used.) Adsorption is accomplished simply by adding a dilute antibody solution to the tube: a considerable amount of the antibody sticks noncovalently, but essentially irreversibly, to the plastic. The remaining components of the assay mixture—tracer, standards, and antigen—are initially present in solution. On their addition to the tubes, the tracer and antigen bind to the antibody, in ratios determined by their relative concentrations. Unbound assay components are subsequently removed, simply by decanting and washing. The radioactivity retained in the tubes is measured, and the data are analyzed as for the classic RIA.

IMMUNORADIOMETRIC ASSAY

The classic RIA is a competition assay, in which excess sample or antigen competes with tracer in binding to a limiting amount of antibody. An immunoradiometric assay (IRMA) is a noncompetitive design in which the antigen itself is the limiting quantity; hence IRMA is in principle orders of magnitude more sensitive than the classical assay (5). An experimentally

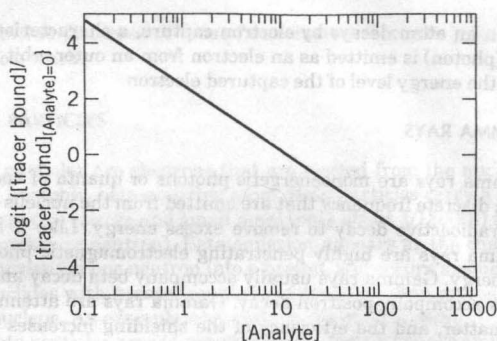


Figure 2. Logit transformation of RIA data from Figure 1. The logit transform converts the S-shaped dose-response curve into a linear form. The advantage of the logit plot is that a straight line is more readily analyzed, and outlying points are more easily identified, than for the direct plot.

important aspect of IRMA is that the antibody is the labeled component of the assay, rather than the tracer. Radiolabeling antibody by **iodination** is technically straightforward and often accomplished more readily than synthesis of labeled tracer (6–9). In the original IRMA method, antigen and labeled antibody are incubated together, and a complex is allowed to form. The mixture is next exposed to an immunosorbent, usually consisting of immobilized antigen, that will complex free antibody through the combining site. The radiolabeled antibody binds, unless it is already binding the antigen. Bivalency of IgG introduces a complication, since one IgG molecule has the ability to bind both antigen and immunosorbent. Nevertheless, measuring the radioactivity in either the solid or solution phase, and comparison of test samples with the standard curve measured using known amounts of antigen, gives an accurate measure of the quantity of antigen in the unknown.

SANDWICH RIA

The sandwich RIA technique (10,11), also known as a “two-site IRMA,” is a solid-phase method that uses two different antibodies, one radiolabeled, to detect a limiting amount of antigen. Both antibodies must be specific for the antigen, but they must bind at independent sites. As a first step, an unlabeled “capture” antibody specific for the antigen is immobilized. (An alternative to using immobilized reagents is to immunoprecipitate the antigen or capture antibody.) Antigen that is unlabeled and free in solution is added and allowed to bind to the capture antibody. Unbound components are washed away. The labeled antibody used for detection is added, and it also binds to the now-immobilized antigen. The unbound detection antibody is washed away, and the radioactivity remaining is measured. The antigen allows a “sandwich” structure to form, and the amount of labeled antibody incorporated into the sandwich is a direct measure of the amount of antigen in the sample.

This assay requires that the two antibody molecules bind to the antigen simultaneously, so the sandwich assay is most appropriate for analysis of **protein** or other large, **macromolecular** antigens. For the sandwich structure to form, the two

antibodies must also bind to nonoverlapping **epitopes** on the antigen, so the use of **monoclonal antibodies** for capture, or for both capture and detection, is advantageous.

BIBLIOGRAPHY

1. S. A. Berson, R. S. Yalow, A. Bauman, M. A. Rothschild, and K. Newerly (1956) *J. Clin. Invest.* **35**, 170–190.
2. R. S. Yalow and S. A. Berson (1960) *J. Clin. Invest.* **39**, 1157–1175.
3. D. Rodbard, P. L. Rayford, J. A. Cooper, and G. T. Ross (1968) *J. Clin. Endocrin. Metab.* **28**, 1412–1418.
4. K. Catt and G. W. Tregear (1967) *Science* **158**, 1570–1572.
5. L. E. M. Miles and C. N. Hales (1968) *Nature* **219**, 186–189.
6. W. M. Hunter and F. C. Greenwood (1962) *Nature* **194**, 495–496.
7. J. I. Thorell and B. G. Johansson (1971) *Biochim. Biophys. Acta* **251**, 363–369.
8. P. J. Fraker and J. C. Speck (1978) *Biochem. Biophys. Res. Commun.* **80**, 849–857.
9. A. E. Bolton and W. M. Hunter (1973) *Biochem. J.* **133**, 529–539.
10. E. Haberman (1970) *Z. Klin. Chem. Biochem.* **8**, 51–55.
11. L. Wide (1969) *Acta Endocrinol. Suppl.* **142**, 207–221.

Suggestions for Further Reading

- A. E. Bolton and W. M. Hunter (1986) in *Handbook of Experimental Immunology*, D. M. Weir, ed., Blackwell, London, pp. 26.1–26.56. (Comprehensive review of RIA methodology.)
- R. Edwards (1997) Radiolabelled immunoassays, in *Principles and Practice of Immunoassay*, C. P. Price and D. J. Newman, eds., Macmillan, London, pp. 325–348.
- D. Rodbard and G. R. Frazier (1975) Statistical analysis of radioligand assay data, *Meth. Enzymol.* **37**, 1–22. (Comprehensive discussion of RIA models, graphic display, and data analysis.)
- R. S. Yalow (1978) Radioimmunoassay: a probe for the fine structure of biologic systems, *Science* **200**, 1236–1245. (Nobel Prize lecture by one of the inventors of RIA.)

RADIOISOTOPES

D. R. FISHER

Isotopes are atomic species of the same atomic number (belonging to the same element) that have different mass numbers. The number of elements in the periodic table is about 110, and each one has more than one isotope; the total number of known isotopes is more than 1500. Each isotope of a given element has the same number of protons in its atomic nucleus, but differs in the number of neutrons in its nucleus. Isotopes of an element cannot be distinguished chemically because they have the same electronic structure and undergo the same chemical reactions.

Although some isotopes are stable, the nuclear configurations of radioisotopes (or radionuclides) are unstable, and they spontaneously undergo a radioactive transformation (or decay) to a more stable energy state (see **Radioactivity**). The half-life of each radioisotope is the time required for exactly one-half of the atoms to undergo radioactive transformation. Radioiso-

topes may decay to either stable or other radioactive species. Decay from one radioisotope to another is called a decay series.

Radioisotopes occur in small amounts in nature as the result of the decay of long-lived primordial materials (such as uranium-238). Atmospheric reactions with solar particles also produce radioactive species. Approximately 50 radionuclides occur naturally in the atmosphere, ocean, or the earth's crust; these include carbon-14, potassium-40, radon-222, radium-226, and uranium-238.

Radioisotopes can be produced artificially by nuclear high energy reactions that combine atomic nuclei. The first human-made or artificial radioisotopes were made by Frederic and Irene Joliot-Curie in 1933, who irradiated a thin aluminum foil with alpha particles and observed tracks in a cloud chamber that diminished in intensity with a half-life of about 3 min, due to phosphorus-30 beta-plus decay. When they replaced aluminum with a boron foil, they found new activity, with a half-life of 14 min, due to nitrogen-13 beta-plus decay (1). In 1934, Lawrence produced small amounts of new radioisotopes at the Berkeley cyclotron using deuteron bombardment reactions on stable-element targets. Fermi produced heavier radioisotopes of the same element by neutron bombardment (or activation), also in 1934 (1). Hevesey conducted the first biological studies with radioisotope tracers. These developments made it possible to discover, produce, and test a large number of scientifically significant radioisotopes during the decade that followed. Radioisotope production continues today. In general, neutron-rich radioisotopes are produced in nuclear reactors, whereas neutron-lean radioisotopes are produced in charged-particle accelerators. A carrier-free radioisotope is one that is not produced or mixed with any other isotope of the same element. The specific activity of a radioisotope preparation is the radioactivity (becquerels or curies) exhibited per unit mass or volume of the radioactive material.

Radioisotopes can be detected easily and identified using radiation detection instruments or photographic film (see **Autoradiography** and **Fluorography**). Therefore, they have numerous practical applications in the physical, chemical, and biomedical sciences. Among the most important applications in biomedical research are those that involve the tagging of a radioisotope to a biomolecule (see **Radiolabeling**) to permit tracking of the molecule in reaction processes and metabolism. Animal tissues containing radioisotopes are analyzed by nuclear radiation-detection techniques such as liquid scintillation counting, gamma spectroscopy, alpha spectrometry, and neutron activation analysis—depending on the relevant radiation emission.

In studies of life processes, the most important radioisotopes are those of **hydrogen**, **carbon**, **sulfur**, and **phosphorous**, because these elements are present in practically all cellular components essential to maintaining life. Some of the more common radionuclides used in biomedical research are given in Table 1, together with their mass number, physical half-life, beta-particle yield and energies, and associated gamma-ray energies.

In molecular biology, the most important application of radioisotopes is the radioactive labeling of nucleic acids and proteins (see **Radiolabeling**). Radioactively labeled cells, such as **organelles** and **chromosomes**, can be imaged on high speed X-ray film in a process called autoradiography.

Table 1. Common Radioisotopes Used in Biomedical Research, with Principal Radioactive Emissions, Yields, and Energies (2)

Element	Mass (amu) ^a	Physical Half-Life	Beta Particle Yield	Average Beta Energy (MeV) ^b	Gamma-Ray Yield	Gamma Energy (MeV)
Hydrogen	3	12.35 years	1.0	0.00568	—	—
Carbon	11	20.38 min	0.998	0.386	2.0	0.511
Carbon	14	5730 years	1.0	0.0495	—	—
Phosphorus	32	14.29 days	1.0	0.695	—	—
Sulfur	35	87.44 days	1.0	0.076	—	—
Calcium	45	163 days	1.0	0.0771	—	—
Iodine	125	59.6 days	—	—	0.0667	0.0355
Iodine	131	8.021 days	1.0	0.182	0.0606	0.284
					0.812	0.364
					0.0727	0.637

^a Atomic mass units.^b Million electronvolts.

BIBLIOGRAPHY

1. M. Brucer (1990) *A Chronology of Nuclear Medicine*, Heritage Publications, Inc., St. Louis, Mo.
2. National Council on Radiation Protection and Measurements (1985) *A Handbook of Radioactivity Measurements Procedures*, 2nd ed., National Council on Radiation Protection and Measurements, Bethesda, Md.

Suggestions for Further Reading

- G. de Hevesey (1961) *Adventures in Radioisotope Research, the Collected Works of George de Hevesy* (2 vols.), Pergamon Press, New York.
- R. D. Evans (1955) *The Atomic Nucleus*, McGraw-Hill, New York.
- J. C. Harbert, W. C. Eckelman, and R. D. Neumann (1996) *Nuclear Medicine: Diagnosis and Therapy*, Thieme Medical Publishers, Inc., New York.
- E. J. Hall (1994) *Radiobiology for the Radiologist*, J. B. Lippincott Co., Philadelphia.
- Y. Wang, ed. (1969) *Handbook of Radioactive Nuclides*, Chemical Rubber Company, Cleveland, Ohio.

RADIUS OF GYRATION

JILL TREWHELLA

The radius of gyration, R_g , is a parameter that can be determined for biological molecules in solution using **small-angle scattering** techniques with X-rays, neutrons, or light. The R_g for a particle is defined as the root-mean-square distance of all elemental scattering volumes from their center of mass weighted by their scattering densities, and it is a simple but useful measure of the overall shape of the particle. R_g values for homogeneous geometrical shapes can be calculated analytically using the relationships in Table 1 (1). These relationships can be very useful in interpreting experimentally determined R_g values. Table 2 shows how R_g values vary for a single protein of a specific molecular weight and partial specific volume, assuming increasingly asymmetric shapes from a perfect sphere to a cylindrical rod. Also shown in Table 1 are the R_g values for a six-subunit assembly assuming various arrangements of the subunits. It is readily seen that R_g gives a simple measure of the asymmetry in a particle. The

mathematical formalisms used for determining R_g values from neutron and X-ray scattering data are somewhat different to those used for **light scattering**. We describe here the conventional equations used in the interpretation of neutron and X-ray scattering data. The formalisms used in **light scattering** are given in its own topic.

DETERMINATION OF R_g FROM SMALL-ANGLE SCATTERING DATA

The **small-angle scattering** of X-rays or neutrons yields the **scattering intensity distribution**, $I(Q)$, which is related to the vector length or pair distribution function by a Fourier transformation:

$$I(Q) = 4\pi \int P(r) \frac{\sin Qr}{Qr} dr \quad (1)$$


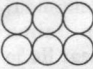
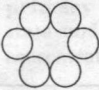
$$P(r) = \frac{1}{2\pi^2} \int I(Q)Q \cdot r \sin(Q \cdot r) dQ \quad (2)$$

Q is the amplitude of the scattering vector, which is equal to $4\pi(\sin\theta)/\lambda$ (λ is wavelength of the scattered radiation, and θ is half the scattering angle). $P(r)$ is the probable frequency distribution of all possible vector lengths, r , between scattering centers (or small volume elements) within a particle, weighted by the product of the scattering densities at the respective centers.

Table 1. Formula for Calculating R_g Values of Simple Geometric Shapes

Sphere radius R	$R_g^2 = \frac{3}{5} R^2$
Hollow-sphere radii R_1 and R_2	$R_g^2 = \frac{3}{5} \frac{R_1^5 - R_2^5}{R_1^3 - R_2^3}$
Ellipsoid, semi-axes a, b, c	$R_g^2 = \frac{a^2 + b^2 + c^2}{5}$
Prism, edge lengths A, B, C	$R_g^2 = \frac{A^2 + B^2 + C^2}{12}$
Elliptic cylinder, semi-axes a, b , height h	$R_g^2 = \frac{a^2 + b^2}{4} + \frac{h^2}{12}$
Hollow cylinder, height h , radii R_1, R_2	$R_g^2 = \frac{R_1^2 + R_2^2}{2} + \frac{h^2}{12}$

Table 2. R_g Values for Various Shaped Objects

	R_g^a (Å)	Maximum Linear Dimension (Å)
Sphere, radius 10 Å, volume 4189 Å ³		
	7.75	20
Prolate ellipsoid, semi-axes 6.325, 6.325, 25 Å, volume 4189 Å ³		
	11.87	50
Cylindrical rod, cross-sectional radius 3.6515 Å, length 100 Å, volume 4189 Å ³		
	28.98	100.27
Different arrangements of six identical spheres, radii 10 Å, total volume 25,134 Å ³		
	35	120
	20.66	~70
	21.44	60

^a R_g values calculated using formulae in Table 1 for the single domain structures, each of which has the same volume. R_g values for the multiple domain structures were calculated using the relationship $R_g^2 = R_{gm}^2 + \frac{1}{N} \sum l_i^2$, where R_{gm} is the radius of gyration of each identical monomer, l_i are the distances of each monomer from the center of mass of the entire assembly, N is the number of monomers, and the sum is over all monomers (6). Note that the lower rosette arrangement has a larger radius of gyration than the rectangular array above it, even though it has a smaller maximum linear dimension. This is because the rosette arrangement has a "hole" in the middle.

R_g can be calculated as the second moment of the pair distribution function $P(r)$:

$$R_g^2 = \frac{\int P(r)r^2 dr}{2 \int P(r) dr} \quad (3)$$

Alternatively, one can determine R_g from scattering data using the Guinier approximation. In 1939 Guinier (2) showed that for sufficiently small Q -values:

$$I(Q) = I(0)e^{-\frac{Q^2 R_g^2}{3}} \quad (4)$$

A plot of $\log [I(Q)]$ versus Q^2 thus yields R_g and the zero angle scatter, $I(0)$, from the slope and intercept, respectively. $[I(Q)]_{Q \rightarrow 0}$ is directly proportional to the square of the molecular weight, M , of the scattering particle. For spherical particles, the Guinier approximation holds for $Q < 1.3/R_g$, and as the scattering particle becomes increasingly asymmetric, the approximation breaks down at even lower Q values.

When one dimension of a particle is much greater than the other two (eg, a rod), Guinier (2) also showed that one can approximate the scattering for certain small- Q values as

$$QI(Q) = I_c(0)e^{-\frac{Q^2 R_c^2}{2}} \quad (5)$$

where R_c is the radius of gyration of cross section $[QI_c(Q)]_{Q \rightarrow 0}$ is directly proportional to the mass per unit length, M_L , of the scattering particle. For a rod of radius R , $R_c = R\sqrt{2}$. The range of Q for which equation 5 is valid depends on the shape of the cross section and the aspect ratio of the rod (3). For infinite cylindrical rods, equation 4 is valid for Q values $< 0.8/R_c$. For finite rods there will be a "rollover" near the origin. Explicitly for rods of radius R and aspect ratio $A = L/2R$, the scattering

intensity will decrease for values of $Q < 5/2AR$ that is, the higher the aspect ratio, the lower the value of Q where the rollover begins. For a rod-shaped object, R_g and R_c are related by

$$R_g^2 - R_c^2 = \frac{L^2}{2} \quad (6)$$

For particles with two dimensions much greater than the third (eg, a disk), the small Q scattering can be approximated as

$$Q^2 I(Q) = I_t(0)e^{-Q^2 R_t^2} \quad (7)$$

where R_t is the radius of gyration of thickness. For a disk of thickness T , $R_t = T/\sqrt{12}$. Equations 5 and 7 break down for particles with low axial ratios, and so they must be used with caution.

Changes in R_g Values Give Insights into Biological Function

In a series of scattering experiments on the dumbbell-shaped calcium-binding protein calmodulin, it was shown that upon binding a wide variety of amphipathic helices, calmodulin undergoes a dramatic conformational collapse involving its two globular lobes coming into close contact. The collapse is facilitated by a flexible helix linking calmodulin's two globular domains, and it is characterized by an approximately 25% reduction in R_g (reviewed in Ref. 4). This conformational flexibility has proven key to understanding how calmodulin binds and activates a wide variety of target enzymes. Another example of the utility of determining R_g values is the study by Mangel et al. (5) in which they characterized an extremely large ligand induced conformational change in native human Glu-plasminogen which was shown to have an R_g value of 39 Å. Upon occupation of a weak lysine-binding site that regulates the activation of plasminogen, the protein's shape irreversibly changes to give an R_g value of 56 Å. This change in shape is achieved without any accompanying change in secondary structure, and the data have been interpreted in terms of a rearrangement of the five domains of the protein structure from a compact, closed structure that is relatively rigid, to an open flexible structure in which the individual domains no longer interact with each other and hence are more accessible. The increased flexibility in the open form is postulated to account for the observation that this form is more readily activated, because it would facilitate urokinase binding. The open form is also proposed to be key to plasminogen's role in fibrinolysis.

BIBLIOGRAPHY

1. P. Mittelbach (1964) *Acta Phys. Austriaca* **19**, 53–102.
2. A. Guinier (1939) *Ann. Phys. (Paris)* **12**, 161.
3. R. P. Hjelm (1985) *J. Appl. Crystallogr.* **18**, 452–460.
4. J. Trehwella (1994) In *Structural Biology: State of the Art*, Vol. I, Proceedings of the Eighth Convention, State University of New York, Albany, 1993 (R. H. Sarma and M. H. Sarma, eds.), Adenine Press, New York, pp. 43–57.
5. W. F. Mangel, B. Lin, and V. Ramakrishnan (1990) *Science* **248**, 69–73.
6. P. Zipper and H. Durchschlag (1980) *Monatsh. Chem.* **111**, 1367–1390.

Suggestions for Further Reading

- C. R. Cantor and P. R. Schimmel (1980) In *Biophysical Chemistry, Techniques for the Study of Biological Structure and Function*, W. H. Freeman, San Francisco, pp. 812–814.
- O. Glatter and O. Kratky (1982) *Small-Angle X-Ray Scattering*, Academic Press, New York.
- A. Guinier and G. Fournet (1955) *Small-Angle Scattering of X-Rays*, Wiley, New York.

RAMACHANDRAN PLOT

JENNIFER MARTIN

The Ramachandran plot is a two-dimensional graph of the phi (ϕ) and psi (ψ) backbone angles for each amino acid residue of a protein; it is a simple method of assessing the quality of a protein structure. It is named after G. N. Ramachandran, who first determined the values of ϕ and ψ that are theoretically permitted (1). The symbols ϕ and ψ are used to represent the dihedral angles of the backbone N–C α ; and C α –C bonds, respectively (Fig. 1). Omega (ω) is the angle of the peptide bond, C–N, but this bond has partial double bond character, so ω can only adopt values close to 180° (called *trans*) or 0° (*cis*). Of these two, the *trans* peptide ω conformation is observed in most cases, unless the following residue is **proline** (see *Cis-trans isomerization*).

The bonds represented by ϕ and ψ are single bonds, and in principle all bond rotations are feasible. Only certain combinations of the backbone angles ϕ/ψ are possible in **polypeptide chains**, however, due to steric restraints imposed by the amino acid **side chains**. These are defined as the most favorable or “allowed” regions of the Ramachandran plot, and they include the **conformations of regular secondary structure** such as α -helix or β -strand. In general, the ϕ angle only adopts negative values. Of the 20 natural amino acids, 18 have only slightly differing allowed values of ϕ and ψ . The **glycine** residue, with only a hydrogen for its side chain, has a high degree of backbone conformational flexibility and can adopt ϕ/ψ angles that are forbidden for other amino acid residues (positive ϕ angles, for example). In contrast, the cyclic nature of the **proline** residue restricts its value of ϕ to approximately –60°.

The residues in natural folded proteins generally adopt fully allowed values of ϕ and ψ ; exceptions usually have functional

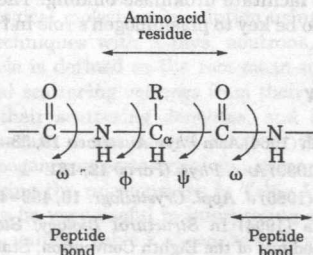


Figure 1. Section of a polypeptide chain showing two peptide bonds (–CONH–) and one amino acid residue (–NH–C α ;(R)(H)–CO–). The functional group R varies, depending on the type of amino acid. The dihedral angles ω , ϕ and ψ of the peptide backbone are labeled.

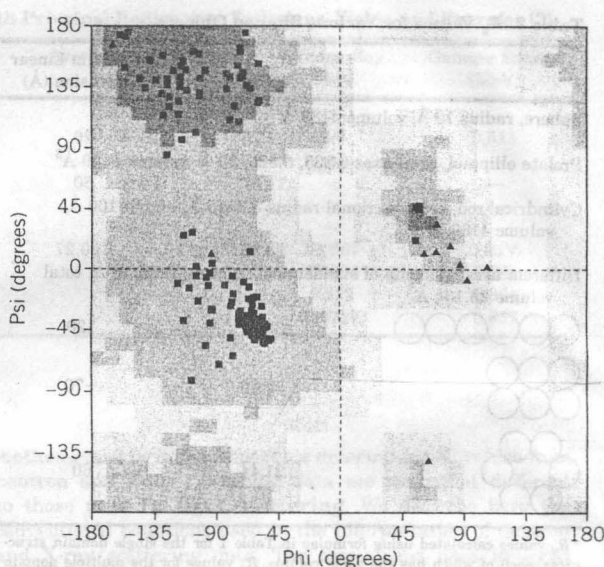


Figure 2. Ramachandran plot for a typical protein structure. The ϕ/ψ values of each nonglycine residue are plotted as squares, and those for glycine residues are shown as triangles. The allowed or most favored regions of the Ramachandran plot are shown in red. The top left section corresponds to β -strand secondary structure, the middle left section corresponds to α -helix and the small middle right section corresponds to left-handed helix. Over 90% of the nonglycine residues fall within the most favored (red) regions of the Ramachandran plot. Additional allowed regions are shown in varying shades of yellow. This figure was generated using Procheck (2). See color insert.

importance. Generally, over 90% of nonglycine amino acid residues in a protein structure have backbone conformations corresponding to the α , β , or turn types of secondary structure. This can be visualized using plots of the observed ϕ/ψ combinations for each residue of a protein structure (Fig. 2). The Ramachandran plot is a very useful means of assessing the quality of a protein structure and of identifying residues with unusual backbone conformations.

BIBLIOGRAPHY

1. C. Ramakrishnan and G. N. Ramachandran (1965) *Biophys J.* 5, 909–933.
2. R. A. Laskowski, M. W. MacArthur, D. S. Moss, and J. M. Thornton (1993) *J. Appl. Crystallogr.* 26, 283–291.

Suggestions for Further Reading

- G. J. Kleywegt and T. A. Jones (1996) Phi/Psi-chology: Ramachandran revisited. *Structure* 4, 1395–1400. (Update on the use of ϕ/ψ plots for protein structure analysis.)
- C. Branden and J. Tooze (1991) *Introduction to Protein Structure*, Garland, New York.
- T. E. Creighton (1993) *Proteins: Structures and Molecular Properties*, W. H. Freeman, and New York.

N. J. Darby and T. E. Creighton (1993) *Protein Structure*, IRL Press, Oxford, U.K.

RANDOM COIL

JENNIFER MARTIN

Random coil describes the multiconformational state of **peptides** and unfolded **proteins** and **polypeptide chains**. In addition, it is sometimes used to refer to the unstructured **conformations** adopted by the **N-terminus**, **C-terminus**, and certain loop regions of stable folded **proteins**. A polypeptide chain in a random coil state adopts multiple interconverting conformations in which the average conformation of each **amino acid residue** is independent of the conformations of all residues other than those immediately adjacent in the **primary structure**. Proteins usually adopt the random coil state under strongly **denaturing** conditions, such as high concentrations of **guanidinium salts** or **urea**.

RANDOM X-INACTIVATION

ALAN P. WOLFFE

It is biologically necessary to make the expression of genes from the two **X-chromosomes** in female cells comparable to that from the single X-chromosome in male cells. To achieve this goal one of the two X-chromosomes in female cells is inactivated (see **X-chromosome inactivation**). The two X-chromosomes from the female cell derive from the male gamete (paternal, X^P) and from the female gamete (maternal, X^M). Both the X^M and X^P chromosomes are functional in the very early female mammalian **embryo**. Once cytodifferentiation starts in the embryonic and extraembryonic tissues of the embryo, however, X-chromosome inactivation occurs (1). In the mouse embryo, the trophectoderm and primitive endoderm preferentially inactivate the paternally contributed X-chromosome X^P . In all other cell lineages that eventually give rise to the adult animal, there is a random inactivation of X^P and X^M (2). This random X-inactivation occurs in all eutherian (placental) mammals, making females functional mosaics of heterozygous X-linked genes. In marsupials, in contrast, the paternally-derived X-chromosome is always inactivated in the female animal (3).

BIBLIOGRAPHY

1. S. G. Grant and V. M. Chapman (1988) *Ann. Rev. Genet.* **22**, 199–217.
2. W. I. Frels and V. M. Chapman (1980) *J. Embryol. Exp. Morph.* **56**, 179–189.
3. G. B. Sharman (1971) *Nature* **230**, 231–232.

RAPAMYCIN

G. FISCHER

Rapamycin (also known as Sirolimus, Rapamune) is a 31-membered macrocyclic lactam **antibiotic** of the **FK506-type** (Fig. 1), isolated from the soil actinomycete *Streptomyces*

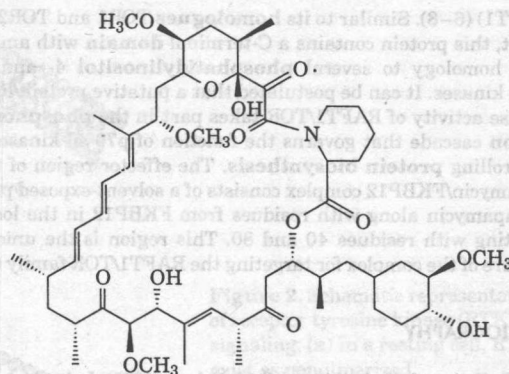


Figure 1. The structure of rapamycin.

hygroscopicus in 1975 (1). The imidic α -ketoacyl-pipecolinyl bond is subject to **cis/trans isomerization**, leading to 38 % *cis* isomer in aqueous solution (2). It was initially evaluated as a potent antifungal agent, but later it was found that it exerts antiproliferative action by disrupting the signaling pathway of **lymphokines** (IL-2, IL-4, IL-6) which promote T cell, B cell, and mast cells. Some nonimmune cell lines are also blocked in proliferation, although rapamycin does not exhibit the properties of a general inhibitor of cell proliferation. The mode of action in these specific effects on the immune response is different from that of the immunosuppressants **cyclosporin A** and **FK506**, in that cells are arrested in the late **G₁ phase**, just prior to the S phase. Moreover, rapamycin suppresses a much wider spectrum of cellular signals. Supporting the belief that it has a pathway distinct from that of other immunosuppressants, only rapamycin inhibits the chronic organ rejection process characterized by graft arteriosclerosis, thus prolonging graft survival. In addition to inhibiting the lymphokine response, the production of antibodies and lymphokines through Ca^{2+} -independent pathway is impaired (3).

Typically, these biological effects are obtained at rapamycin levels (picomolar to micromolar) below those at which it is toxic. Rapamycin does not always act synergistically with cyclosporin A and FK506, as in the inhibition of T cell and B cell proliferation, but it often affects identical intracellular signaling events (4). Sometimes, FK506 and rapamycin reciprocally antagonize the parameters tested, suggesting a common cellular receptor for both compounds. Indeed, at doses in the picomolar range of concentration, both drugs bind reversibly to FK506-binding proteins (FKBP). Among mammalian FKBP, the cytosolic FKBP12 is responsible for mediating rapamycin effects (5). Binding always occurs with a concomitant inhibition of the **peptidyl prolyl cis/trans isomerase** (PPIase) activity of the FKBP, but this inhibition fails to account for the immunosuppressive effects. Instead, several lines of evidence show an indirect positive action of the rapamycin/FKBP12 complex, because rapamycin treatment induces the inhibition of several cellular serine/threonine **kinases**, including mammalian p70 S6 kinase.

The upstream target, which may represent the protein that physically interacts with the drug/receptor complex, is the 289-kDa **RAFT1** protein in mammals (also known as **FRAP** or